Optical and Quantum Electronics (2023) 55:453
https://doi.org/10.1007/s11082-023-04746-4

Optical strain sensor with dual fibre Bragg grating topology

Jacek Palmowski[1] · Kamil Barczak[2] · Natalia Kubicka[3] · Franek Gołek[4] · Luke Benson[5] · Erwin Maciak[2] · Tadeusz Pustelny[2] · Sendy Phang[6] · Trevor Benson[6] · Elżbieta Bereś-Pawlik[1,6]

Received: 12 January 2023 / Accepted: 3 March 2023 / Published online: 27 March 2023

Abstract
The paper presents the design, operation, and proof of principle realisation and validation of a relatively cheap fibre optic strain sensor based on two fibre Bragg grating (FBG) elements with different spectral responses. Its performance is compared with the measurement capabilities of a FBG-based sensor that uses an optical interrogator.

Keywords Fibre Bragg gratings · Fibre optic sensing · Optical interrogator · Strain measurement · Environmental sensing

1 Introduction

Issues related to building sensory networks have interested researchers for many years. Fibre Bragg gratings (FBGs) are especially popular and can be used to measure stress, vibration, temperature, and humidity. Sometimes it is important to measure several parameters simultaneously with the use of FBGs, or to measure one parameter in many places. It is then necessary to build sensor networks arranged in series or in parallel. Sensory network systems are discussed in many works, for example (Chan et al. 2000; Allwood et al. 2019; Bhaskar et al. 2021). The possibility to multiplex sensors and/or transmit data over long distances using fibre optic networks, combined with their inherent immunity to external electromagnetic fields, gives fibre optic sensors advantage over

✉ Elżbieta Bereś-Pawlik
elzbieta.berespawlik@gmail.com

1 RELS Limited, ui. Warciańska 18, 54-128 Wrocław, Poland

2 Faculty of Electrical Engineering, Silesian University of Technology, ui. Krzywoustego 2, 44-100 Gliwice, Poland

3 Faculty of Electronics and Information Technology, Warsaw University of Technology, ui. Nowowiejska 15/19, 00-665 Warsaw, Poland

4 Institute of Experimental Physics, University of Wroclaw, Plac Maksa Borna 9, 50-204 Wrocław, Poland

5 School of Physics and Astronomy, University of Leeds, Woodhouse Lane, Leeds LS2 9JT, UK

6 Faculty of Engineering, George Green Institute for Electromagnetics Research, University Park, University of Nottingham, Nottingham NG7 2RD, UK

popular electronic sensors based on resistive, capacitive, and piezoelectric properties. Using an optical network incorporating fibre optic sensors it is possible, for example, to continuously monitor the movements of rock masses in mines in terms of stress or seismic displacement or the humidity of forest areas and vineyards (Allwood et al. 2019).

Sensor systems using FBGs presented in the literature allow one to measure various parameters, including temperature, humidity, vibration, or strain (Kersey et al. 1997; Grattan and Sun 2000; Wild and Richardson 2015; Mądry et al. 2016; Bereś-Pawlik and Mądry 2018). Usually, such a measurement uses a single sensor (Wild and Richardson 2015; Mądry et al. 2016) and interrogator systems. These interrogators measure the shift of the transmission or reflection spectrum of a FBG under the influence of external factors. Interrogators are commercially available; however, they are not cheap. This paper presents the development of a sensor system in which changes in the parameter to be monitored are determined by measuring only the change in the output power from an optical system containing a sensing FBG; this can be converted to a voltage output by additionally using a widely available and easy-to-use, operational-amplifier-based, current-to-voltage convertor. The simplicity of the proposed solution, which measures power rather than the shift of the maximum spectrum, is emphasised. Such a sensor placed in branch of an optical fibre network can be characterised by low cost, easy installation, and the reliability and repeatability of measurements. The concept of using dual FBGs is similar to that reported by (Takahashi et al., 2001) but there are some important differences. As in the present work, Takahashi et al. used a combination of a circulator and FBG to produce a narrow-spectrum light source for the sensor FBG. However, in (Takahashi et al., 2001) the wavelength of this reference corresponded to the slope of the reflection spectrum of the test FBG such that the reflected light intensity was intensity modulated as the reflection spectrum of the test FBG changed. (Pachava et al., 2015) described a similar low-cost FBG-based interrogation system that was used for pressure sensing. It included a long period grating (LPG) as a linear edge filter. The LPG interrogation scheme converted the wavelength information of the measurement FBG into equivalent intensity modulated signals that were detected by a simple photodiode. The FBG pressure sensor was compensated using a reference FBG temperature sensor, enabling a resolution of up to 0.025psi to be experimentally achieved. (Xu et al., 2017) used two FBGs in series to generate two passbands in a dual-frequency opto-electronic oscillator (OEO) and used the beating between OEO-generated microwave signals to cancel the frequency shift due to temperature change. High resolution sensing with a resolution of 0.83 microstrain was experimentally demonstrated.

The paper presents results for the illustrative example of an FBG-based strain sensor. Traditional interrogator-based measurements are also made and compared with the theoretical and experimental results for the proposed strain sensor which it is re-emphasised uses only a measurement of guided optical power. In the work, we compare the measurement capabilities of the traditional and the newly proposed methods. The remainder of the paper is structured as follows. Section 2 describes the proposed measuring system. Section 3 presents more details on the mechanical system used to introduce strain into the test FBG in the present work. Its performance is evaluated using an interrogator which provides a useful framework for further discussions. Section 4 shows experimental results for the proposed sensor system. Section 5 describes theoretical considerations and provides a comparison of the experimental results of the proposed method with calculated results to establish and validate the principle of operation. Section 6 presents the conclusions from the work.

2 Overview of the proposed measuring system

Figure 1 shows the proposed measurement system, together with arrows that indicate the paths of the rays considered. The dashed arrows indicate the rays reflected from the two FBGs. The solid arrows illustrate rays that are transmitted by the FBGs. The dot-dash arrow shows those rays reflected from the reference FBG (G1) that enter the strained FBG considered (labelled as G).

The following elements were used in the proposed measuring system:

- A WT&T model LE-3BB broadband light source with a nominal centre wavelength of 1550 nm and a full width half-maximum (FWHM) ≈ 40 nm at the maximum optical power of + 10.1 dBm (https://www.wttechnology.com/).
- A fibre-based optical circulator with a nominal insertion loss between ports 1–2 and 2–3 of 0.8 dB.
- FBGs G1 (reference) and G (strained) are silica-based fibres manufactured by Safibra, https://safibra.com/. The unstrained reflection spectra of the two FBGs were measured before use on a YOKOGAWA AQ6374 Optical Spectrum Analyser (OSA). The measured spectra are presented in Fig. 2, where the plots are each normalised to the manufacturer's quoted maximum reflectivity. For FBG G1 this maximum reflectivity is 0.9369, and for FBG G it is 0.9624. These two FBGs were already available in our laboratory and were chosen for the present proof of principle experiments because of their large bandwidth and close central wavelengths.
- FC / APC fibre connectors.
- Detector: PD-10-FA InGaAs PIN photodiode with a particularly low dark current (http://www.oemarket.com/). This was used in conjunction with an OP-AMP based current–voltage converter (Millman and Halkias 1972) to obtain an output voltage that is proportional to the detected power.

The operation of the sensor is based on the combination of two of these fibre FBGs, the reference one labelled as G1 in Fig. 2 and the measuring (strained) one labelled as G in Fig. 2.

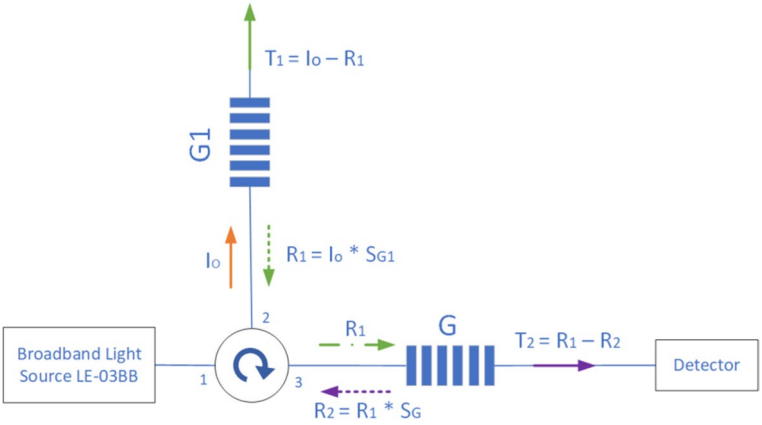

Fig. 1 Schematic of the measuring system proposed, together with arrows which indicate rays considered in the calculation of the power detected by the detector. G1 is a reference FBG; G is the sensing FBG which in the present implementation is strained

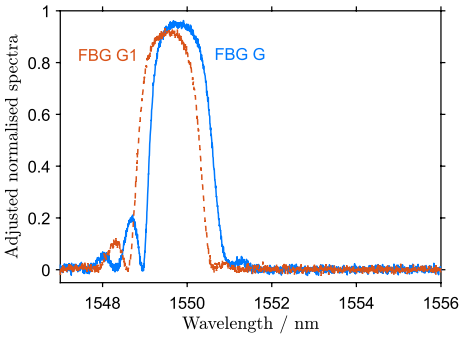

Fig. 2 Individually measured unstrained reflection spectra for the two FBGs used in the experiments. The measurements were made using a YOKOGAWA AQ6374 Optical Spectrum Analyser and normalised to the manufacturer's quoted maximum reflectivity for each FBG

The reference FBG G1 works in reflection mode. The measurement FBG G is subjected to strain (the illustrative environmental factor measured in this paper) and works in transmission mode. This is discussed further in Sects. 3 and 4.

3 Description of the mechanical system for introducing strain into a fibre Bragg grating and its evaluation using an interrogator

The specially constructed stand with a micrometre screw shown in Fig. 3 was used to introduce strain into the fibre Bragg grating G. The strained fibre Bragg grating was mounted in the two outermost fibre optic holders. By changing the position of the micrometre screw, stretching of the FBG was introduced, which emulates tensile strain that might be experienced by the FBG in a practical sensing environment. The unstretched length of fibre G between the fibre holders was 18 cm.

The performance of the mechanical system was evaluated using a Sylex S-Line Scan 400 interrogator and FBG G. This evaluation is presented now to aid the further discussion of the proposed system in Sects. 4 and 5. As the tensile strain is increased, the wavelength of maximum reflection for the FBG G shifts towards higher wavelength values, see Figs. 4 and 5. Spectral shift changes were measured up to a total displacement of 0.52 mm, in steps of 0. 04 mm. It is expected that the observed shift in the reflection spectrum would increase further with further applied strain up to the elastic limit of the FBG. Figure 4 shows the change in the reflection spectrum of FBG G, measured using the interrogator, as it is extended by 0.12, 0.24, 0.36 and 0.48 mm to introduce tensile strain. The spectrum for zero extension is indistinguishable from that shown for a nominal extension of 0.12 mm. Referring to Fig. 4, FBG G has a broad main reflection peak and several sharper secondary reflection peaks are visible at lower wavelengths on this logarithmic scale. Figure 5 presents two plots, one for the shift of the wavelength position of the main peak with extension, and one for the wavelength

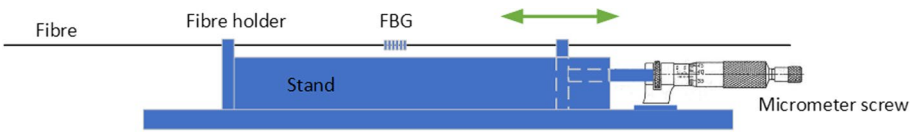

Fig. 3 Mechanical system for stretching a fibre Bragg grating (FBG)

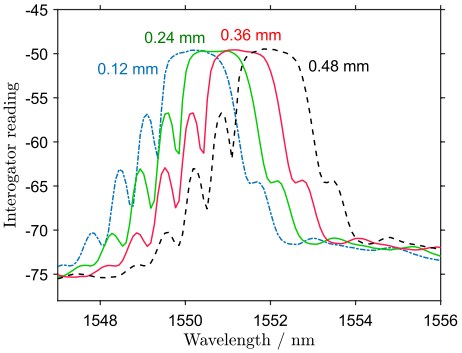

Fig. 4 Change in the reflection spectrum of FBG G, measured using a Sylex S-Line Scan 400 interrogator, as it is extended by 0.12, 0.24, 0.36 and 0.48 mm to introduce tensile strain. The spectrum for zero extension is indistinguishable from that shown for a nominal extension of 0.12 mm

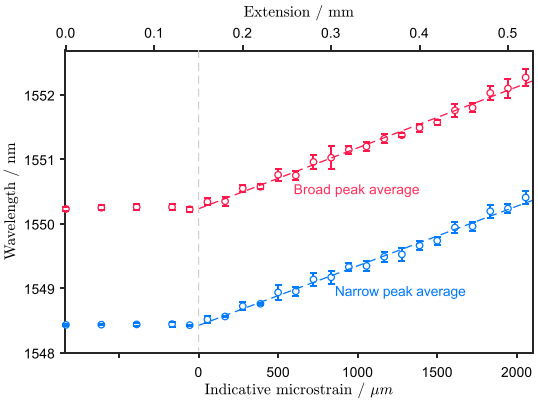

Fig. 5 Measurements of the peak wavelength of the main and one of the secondary reflections of FBG G as a function of extension from the reference position. The indicative microstrain shown is referenced to zero strain being at the extension of 0.15 mm for which a shift in the reflection spectrum was first observed

position of a secondary peak, which proved easier to determine as the peak was narrower. Each plot in Fig. 5 shows the average and standard deviation of five measurements. FBG G was not removed from the mechanical system between the measurements presented in Figs. 4 and 5 and those presented for the proposed system when using FBG G in Sects. 4 and 5.

The measurements shown in Fig. 5 suggest that the spectrum of FBG G starts to shift when the applied extension increases above about 0.15 mm from the mounting reference point taken to be zero extension. This is commensurate with the observation that the fibre sagged slightly in the mount at the reference point and then became taught when a further slight extension was applied. The data shown in Fig. 5 was fitted to straight line plots shown for extensions above 0.15 mm. These have gradients of 5.3 nm/mm and 5.1 nm/mm for the broad and narrow peaks respectively with R2 (the square of the value of the correlation coefficient) values of 0.992 and 0.993, respectively. The unstrained fibre length between the holders was 18 cm. Indicative microstrain is also indicated in Fig. 5. This is referenced to zero strain being at the extension of 0.15 mm for which a shift in the reflection spectrum was first observed. The gradients of 5.2 nm/mm and 5.1 nm/mm respectively correspond to sensitivities 0.94 pm per microstrain and 0.92 pm per microstrain. This sensitivity is similar to that reported by (Guan et al. 2000). The quoted measurement accuracy of the interrogator used in our experiments is ± 20 pm, such that in principle changes of the order 21–22 microstrain can be measured.

4 Experimental results for the proposed measuring system

The measured values of voltage (proportional to detected power) are shown as a function of extension for a broadband source power of − 14.02 dBm in Fig. 6. The unstretched length of fibre G between the fibre holders was 18 cm. The results shown are the average of five independent sets of measurements, each set taken whilst increasing and then decreasing the extension, and the error bars shown on the figure indicate the standard deviation of the measurements.

The results presented in Fig. 6 confirm that it is possible to convert changes in the optical signal arising from the influence of environmental changes (here strain) into a voltage signal representative of the output power measurement. This is extremely useful in practice because this voltage can subsequently be digitised using an Analogue to Digital convertor (ADC) and subsequently processed. For example, it may be sent it to a centre monitoring a change of strain in a mine.

Figure 6 shows that the proposed strain sensor can determine changes in strain over the range of extensions from around 0.15 to 0.42 mm. Whilst the corresponding range of indicative microstrain of 0 to 3000 microstrain (με) may seem small, there are mechanical means by which a strain to be evaluated can be adjusted to the range that can be measured using the FBG (Shiryayev et al. 2022). Interestingly, the proposed strain sensor also provides a well-defined constant voltage level for larger extensions.

The reflection spectrum of a FBG is dependent on temperature; the experimental results presented in Figs. 5 and 6 were collected under laboratory conditions over a period of a few hours; changes in temperature and humidity were not monitored but were not noted to vary significantly over this period. It is estimated from the measured data presented in (Kersey et al. 1997) that at wavelengths around 1550 nm the thermal responsivity at constant strain is of the order of 0.01 nm per °C. The largest standard deviations observed in the measurements presented in Fig. 5 are of the order of 0.1 nm. These are thought to arise because of mechanical uncertainly in the applied extension, rather than temperature changes, which is supported by the observation that the standard deviation of the measurements is an order of magnitude smaller in the region where the applied extension is below 0.15 mm, where the fibre sagged slightly in the mount and the indicative strain is zero.

Optical fibre grating based sensors for relative humidity measurement typically use a fibre coating that experiences a change of its physical and optical properties as a result of the absorption of moisture. This subsequently modifies the characteristic spectral features of the fibre grating used, see for example (Alwis et al. 2013). No such coating was applied

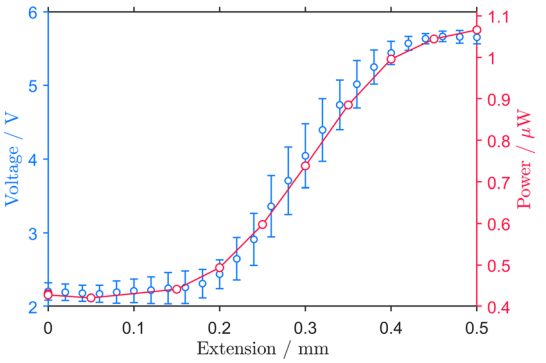

Fig. 6 Measured values of the output voltage proportional to transmitted power in the sensor system of Fig. 2 using FBGs G1 (reference) and G (strained element) for an input power level of − 14.02 dBm. The experimental results are compared to calculations based on Eq. (1) presented in Sect. 5 taking to account the shift in the reflection spectrum of FBG G as it is extended

to the FBGs used in the present proof of principle experiments and so the influence of humidity on our measurements is expected to be negligibly small.

5 Theoretical considerations

The measurement setup shown in Fig. 1 works as follows. The source of the measurement signal is an incoherent broadband light source LE-3BB operating in the near-infrared. The radiation beam is directed by the optical circulator towards the reference grating (G1), port 1 and the signal reflected from this is directed by the circulator to port 2. Part of the signal reflects off the reference FBG (G1) and returns towards the circulator to port 2 with the spectrum of the form shown in Fig. 2. This is fed into the strained FBG (labelled as G) by the circulator. FBG G works in transmission mode; it thus essentially 'blocks' that part of the reference signal that overlaps with its reflection spectrum from reaching the detector. Following the above discussion, the output/input ratio depends on the shape and spectral widths of the pair of FBGs used. This value is the highest for FBGs with similar spectral widths and central wavelengths under the zero-strain condition, such that the test FBG G reflects all the reference spectrum provided by FBG G1 at zero strain but allows all of it to pass in the limit when its reflectance spectrum falls outside of that of the reference.

As the tensile strain is increased, the wavelength of maximum reflection for the FBG G shifts towards higher wavelength values, see Figs. 4 and 5. This results in a decrease in the common area under the spectral curves for FBGs G1 (the reference) and G (the strained element). Consequently, there is an increase in the transmission of the guided signal. This increased transmission leads to an increase in the value of the detector photocurrent and the output voltage of the current to voltage (I to V) convertor. The photocurrent of the detector and the voltage output of the I to V convertor will change in proportion to the output optical power, provided the photodiode has zero dark current, the amplifier has zero offset, and all is linear.

The transmitted optical power reaching the detector was calculated according to the formula (1):

$$P_{OUT} = \int T_2(\lambda)d\lambda = \int R_1(\lambda)d\lambda - \int R_2(\lambda)d\lambda = \int I_o(\lambda)S_{G1}(\lambda)d\lambda - \int I_o(\lambda)S_{G1}(\lambda)S_G(\lambda)d\lambda \tag{1}$$

where, in the notation of Fig. 1, *Io(λ)* is the spectral power density (mW/nm) of the broadband light source, T_2 (λ) is the spectral power density transmitted by FBG G, $R_{1,2}$ are spectral power densities reflected by FBGs G1 and G respectively, *SG1* (λ) is the power reflection spectrum of FBG G1, and SG (λ) is the reflection spectrum of the strained FBG G. The explanation of the formula (1) is presented in Fig. 1. The integrations in Eq. (1) were carried out numerically over the wavelength from 1547 to 1560 nm using a trapezoidal rule and the spectra data of the broadband source at the power level used, of FBG G1 (reference), and of FBG G for the various values of applied strain individually measured using the YOKOGAWA AQ6374 Optical Spectrum Analyser. The integration step used for the trapezoidal rule integration was the wavelength separation of 0.0004 nm used for recording the spectral data using the YOKOGAWA AQ6374 Optical Spectrum Analyser. The optical losses introduced by the circulator and other optical components were neglected in these calculations.

Figure 6 compares the results calculated using Eq. (1) for the combination of FBGs G1 and G with the experimental results. Excellent agreement is observed. For extensions

between 0.2 and 0.4 mm the calculated sensitivity of the system is 4.52×10^{-4} μW per microstrain. A compressive strain applied to the test FBG G would move its wavelength of maximum reflection towards lower wavelength values, but this could not be realised using the simple mechanical system shown in Fig. 3. In the case of compressive strain, the common area under the spectral curves for FBGs G1 (the reference) and G (the strained element) will, after an initial increase, again decrease, resulting in an increase in the detected power.

6 Conclusions

The paper presents a new method of strain measurement with the use of two FBGs, one of which is used to provide a reference input signal. The method allows the construction of relatively cheap sensors for measuring changes in environmental parameters, in this illustrative case changes in strain, and measuring these parameters through convenient power measurements. The relative cheapness arises because the proposed sensor avoids the use of an interrogator. The study compares the results obtained with the proposed sensor with the results obtained by a traditional method using of an interrogator. The proposed sensor operates over a smaller measurement range than when using an interrogator, but it has the potential benefit for environmental monitoring applications of producing a constant output level above a threshold value. The measurement range might be increased by using FBGs with broader spectral characteristics to those presented here. This suggests that in future work the use of the broader spectrum of a long period grating may beneficial.

The illustrative proof of principle experiments described simplistically emulate tensile strain that might be experienced by the FBG in a practical sensing environment using the specially constructed stand shown in Fig. 3. For practical application, the test FBG will require specialist mounting, using suitable adhesives, bonding, or welding, and subsequent calibration and fatigue testing. Sensor packaging and installation can require suitable protective coatings and housings for fibre sensors, especially those operating in harsh environments, and detailed knowledge on the transfer of the properties to be monitored (strain, temperature, etc.) from the specimen under test to the sensing fibre (Wnuk et al. 2005).

Acknowledgements TMB acknowledges, with thanks, the financial support of a Leverhulme Emeritus Fellowship, reference EM-2022-028.

Authors' contributions Experimental work was undertaken by JP, KB, NK, FG, LB, EM, TP, TB, and EB-P. Calculations were performed by JP, SP, NK, TB, and EB-P. EB-P, TB, JP, SP, and LB wrote the main manuscript text, undertook data analysis, and prepared figures. All authors reviewed the manuscript.

Funding TB was funded by an Emeritus Fellowship from The Leverhulme Trust, Grant reference EM-2022-028.

Data availability Contact Professor Dr Beres-Pawlik, elzbieta.berespawlik@gmail.com.

Declarations

Conflict of interest The authors declare that there is no conflict of interest.

Ethical approval Not applicable. No human and/or animal studies.

References

Allwood, G., Richardson, S., Wild, G., Hinckley, S.: Standardization of FBG sensors in dual-bus fiber networks. In: AOS Australian Conference on Optical Fibre Technology (ACOFT) and Australian Conference on Optics, Lasers, and Spectroscopy (ACOLS) 2019 (Vol. 11200, pp. 175–176). SPIE (2019)

Alwis, L., Sun, T., Grattan, K.T.V.: Design and performance evaluation of polyvinyl alcohol/polyimide coated optical fibre grating-based humidity sensors. Rev. Sci. Instrum. **84**, 025002 (2013). https://doi.org/10.1063/1.4789768

Bereś-Pawlik, E., Mądry M.: Polish Patent. Fiber optic system for monitoring changes in the physical size of materials. 227634. (2018)

Bhaskar, C.V.N., Pal, S., Pattnaik, P.K.: Recent advancements in fiber Bragg gratings based temperature and strain measurement. Results Opt. **5**, 100130 (2021)

Chan, P.K., Jin, W., Demokan, M.S.: FMCW multiplexing of fiber Bragg grating sensors. IEEE J. Sel. Top. Quantum Electron. **6**(5), 756–763 (2000)

Grattan, K.T.V., Sun, T.: Fiber optic sensor technology: an overview. Sens. Actuators, A **82**(1–3), 40–61 (2000)

Guan, B.-O., Tam, H.-Y., Ho, S.-L., Chung, W.-H., Dong, X.-Y.: Simultaneous strain and temperature measurement using a single fibre Bragg grating. Electron. Lett. **36**(12), 1018–1019 (2000)

Kersey, A.D., Davis, M.A., Patrick, H.J., LeBlanc, M., Koo, K.P., Askins, C.G., Putnam, M.A., Friebele, E.J.: Fiber grating sensors. J. Lightwave Tech. **15**(8), 1442–1463 (1997)

Mądry, M., Markowski, K., Jędrzejewski, K., Bereś-Pawlik, E.: Power modulated temperature sensor with inscribed fibre Bragg gratings. Opto-Electron. Rev. **24**(4), 183–190 (2016)

Millman, J., Halkias, C.C.: Integrated electronics: analog and digital circuits and systems, p. 540. McGraw Hill, International Student Edition (1972)

Pachava, V.R., Kamineni, S., Madhuvarasu, S.S., Putha, K., Mamidi, V.R.: FBG based high sensitive pressure sensor and its low-cost interrogation system with enhanced resolution. Photonic Sens. **5**, 321–329 (2015)

Shiryayev, O., Vahdati, N., Yap, F.F., Butt, H.: Compliant mechanism-based sensor for large strain measurements employing fiber optics. Sensors **22**, 3987 (2022). https://doi.org/10.3390/s22113987

Takahashi, N., Yoshimura, K., Takahashi, S.: Fiber Bragg grating vibration sensor using incoherent light. Jpn. J. Appl. Phys. **40**, 3632–3636 (2001). https://doi.org/10.1143/JJAP.40.363

Xu, O., Zhang, J., Deng, H., Yao, J.: Dual-frequency optoelectronic oscillator for thermal-insensitive interrogation of a FBG strain sensor. IEEE Photonics Technol. Lett. **29**(4), 357–360 (2017)

Wild, G., Richardson, S.: Analytical modeling of power detection-based interrogation methods for fiber Bragg grating for system optimization SPIE. Opt Eng **54**(9), 097109 (2015)

Wnuk, V.P., Méndez, A., Ferguson, S., Graver, T., 2005, Process for mounting and packaging of fiber Bragg grating strain sensors for use in harsh environment applications. In: *Smart Structures and Materials 2005: Smart Sensor Technology and Measurement Systems* (Vol. 5758, pp. 46–53). SPIE. (2005)